Rainfall Estimation in the Sahel: What Is the Ground Truth?

THIERRY LEBEL AND ABOU AMANI

IRD, LTHE, UMR, Grenoble, France

(Manuscript received 15 December 1997, in final form 10 July 1998)

ABSTRACT

Areal rainfall estimation from ground sensors is essential as a direct input to various hydrometeorological models or as a validation of remote sensing estimates. More critical than the estimation itself is the assessment of the uncertainty associated with it. In tropical regions knowledge on this topic is especially scarce due to a lack of appropriate data. It is proposed here to assess standard estimation errors of the areal rainfall in the Sahel, a tropical region of notoriously unreliable rainfall, and to validate those errors using the data of the EPSAT–Niger experiment. A geostatistical framework is considered to compute theoretical variances of estimation errors for the event-cumulative rainfall, and rain gauge networks of decreasing density are used for the validation. As a result of this procedure, charts giving the standard estimation error as a function of the network density, the area, and the rainfall depth are proposed for the Sahelian region. An extension is proposed for larger timescales (decade, month, and season). The seasonal error is estimated as a product of the error at the event scale by a reduction coefficient, which is a function of the number K of recorded events and the probability distribution function of the point storm rain depth. For a typical network of 10 stations regularly dispatched over a $1^\circ \times 1^\circ$ square, the relative estimation error decreases from 14% for an average storm rain depth of 16 mm to 5% for an average August rainfall of 160 mm. For a density comparable to that of the operational rain gauge network of southern Niger and similar Sahelian regions, the standard errors are, respectively, 26% at the event scale and 10%–15% at the monthly scale, depending on the number of events recorded during the month. The areas considered here are $1^\circ \times 1^\circ$ and smaller, which makes a comparison with results obtained in previous studies for other regions of the world difficult since the reference area most often used in these studies is either $2.5^\circ \times 2.5^\circ$ or $5^\circ \times 5^\circ$. Further work is thus needed to extend the results presented here to larger spatial scales.

1. Introduction

Even though it is very basic to any hydrological study and, as such, has been a subject of research for several decades, rainfall estimation remains an elusive issue. This is especially true in tropical regions where rainfall is highly variable in space and time, due to its convective origin, and where ground-based rain measurements are scarce. Rainfall estimation in the Tropics is important for a number of reasons. Two of them, one global and one regional, are central to this paper.

1) Tropical convection plays a major role in the global energy and water budgets of the planet. Thus, a better understanding and modeling of the earth's climate requires estimates of tropical rainfall as precise as possible. Two large international experiments focused on the tropical climate, TOGA COARE and HAPEX-Sahel, both had a strong rainfall estimation component.
2) The two main biomes of the continental Tropics are the tropical forests and the savannas, accounting for 15×10^6 and 14×10^6 km^2, respectively (Le Roux et al. 1994). The tropical savannas are regions where the potential evapotranspiration is much higher than the rainfall, both at the annual and monthly scales, except for a few short periods during the core of the rainy season. Any significant decrease of the rainfall will thus impact sharply onto the vegetation and the living conditions of the local populations. This is exactly what has been observed for the past 25 years over the Soudano-Sahelian part of West Africa, where savannas cover 3×10^6 km^2 (all in one block). Ongoing hydrological, bioclimatological, and agronomical studies carried out to assess the impact of this drought onto the regional water budget are all facing the question of how reliable are the rainfall inputs to the models used for such studies.

Among the means developed by the scientific community to remedy to the lack of adequate measurements over the Tropics, and especially over tropical Africa, which is, by in large, the greatest piece of tropical land, are satellite missions designed to test rainfall estimation algorithms based on spaceborne microwave sensors. Two such missions are currently considered: the Tropical Rainfall Measuring Mission (Simpson et al. 1988)

Corresponding author address: Dr. Thierry Lebel, IRD, Groupe CATCH, LTHE, BP 53, 38041 Grenoble, Cedex 9, France.
E-mail: thierry.lebel@hmg.inpg.fr

and TROPIQUES (Desbois 1994). Sampling problems associated with these missions are of two types. First, one must assess the accuracy of the so-called ground truth used to validate rainfall satellite algorithms. This is essentially a spatial sampling problem linked to the interpolation of ground point measurements. Second, there is a time sampling problem related to the time frequency of satellite passes over a given region.

In this paper we will address only the space sampling question. Several studies have been devoted to this question over the recent years, as will be examined in section 2. The study presented here has some specific features that will advance previous works.

- It focuses on the Sahel, where rainfall is notoriously unreliable and drought has had its most drastic consequences during the past two decades.
- It is centered on an experimental validation of modeling results from a high space–time resolution dataset, the best of its kind over tropical Africa.
- It covers an array of scales from the event to the seasonal scales in time and from 100 to 10 000 km^2 in space.

2. A Sahelian case study

a. A brief review of the literature

Let k be a rainfall event recorded by a rain gauge network composed of N gauges and $P_{i,k}$ ($i = 1, \ldots, N$) the cumulative precipitation observed at the different gauges. The areal precipitation $P_k(A)$, over a given area A, is

$$P_k(A) = \frac{1}{A} \int_A P_k(x, y)\, dA, \tag{1}$$

where $P_k(x, y)$ is the rainfall depth at point with coordinates (x, y). Here, $P_k(A)$ is generally estimated as a linear combination of the recorded rain depths

$$\hat{P}_k(A) = \sum_{i=1}^{N} \lambda_i P_{k,i}, \tag{2}$$

where $\{\lambda_i\}$ is the set of weights associated to a given network configuration. In a stochastic framework, $\hat{P}_k(A)$ is considered as a random variable. Its variance of estimation error is defined as

$$\sigma_k^2(A) = E\{[P_k(A) - \hat{P}_k(A)]^2\}. \tag{3}$$

Computing $\sigma_k(A)$ is a way of evaluating the estimation accuracy of $P_k(A)$. This question has been addressed by various authors whose methods largely depended on the region of study and the scales concerned. Indeed there has been a sustained interest in that issue over years for one major reason: rainfall is central to any water budget calculation, whether in a purely hydrologic perspective or in the framework of atmosphere–land surface interactions.

A pioneering work was the experimental study of Huff (1970), based on a dense network of 49 gauges spread over a 1000 km^2 (400 mi^2) area. No explicit modeling of the spatial structure of the rain fields was carried out. Results were believed to be representative for ''the Midwest and other areas of similar precipitation climate.'' Most of the following studies involved a modeling of the spatial covariance function of the rainfields either directly (e.g., Zawadzki 1973; Rodriguez-Iturbe and Meija 1974; Lebel et al. 1987; Li et al. 1996; Morissey et al. 1995) or through a spectral approach (e.g., North and Nakamato 1989; Graves et al. 1993; Valdes et al. 1994). Other modeling approaches include isohyet-area models (Silverman and Rogers 1981) or simulations from conceptual stochastic space–time models of rainfall (Bell et al. 1990; Peters-Lidard and Wood 1994). Experimental studies have been less numerous and mostly based on radar data (e.g., Silverman and Rogers 1981; Seed and Austin 1990). Woodley et al. (1975) take advantage of the dense setup of Florida Area Cumulus Experiment to compare rain gauge and radar estimates. Flitcroft et al. (1989), used a network of 36 nonrecording rain gauges covering 100 km^2 to relate point to areal rainfall in northern Niger.

Generally, the estimation error is given as a function of some, or all, of the following criteria: 1) the area of estimation, 2) the number of gauges, 3) the geometry of the rain gauge network, 4) the spatial structure of the rainfall, 5) the mean rainfall depth, and 6) the time of accumulation (but most studies concentrate on the storm or event rainfall). Huff (1970) has pointed out that this error also depends on the type of rainfall events, the meteorological conditions, and the season.

b. The EPSAT–Niger dataset

The brief review of literature given above, even though not comprehensive, shows that very few studies have focused on the continental tropical areas (and only one on the Sahel, that of Flitcroft et al. 1989) despite their importance for the climate of the planet and the fragility of their water resources. The issue is most crucial in the case of the Sahel, for rain gauge networks are especially sparse there and thus the reliability of the rainfall estimates based on them must be investigated. Also, most modeling studies were not sustained by a validation procedure (data are used only to calibrate the covariance or conceptual models), which, for tropical rainfall, is easily explainable by the lack of appropriate ground data.

The EPSAT–Niger (E–N) dataset (Lebel et al. 1995) provides a first opportunity to conduct a modeling study of the rain field correlation function in tropical Africa, as upheld by a validation study. This is important because 1) empirical relationships derived from experimental studies cannot cover the full spectrum of sampling possibilities and 2) estimation errors derived from models without validation leave open the question of the validity of the model used. The high resolution, both

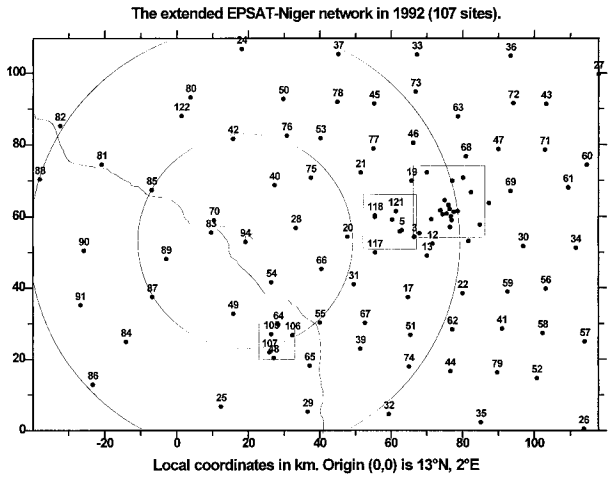

FIG. 1. The EPSAT–Niger recording rain gauge network.

in space and time, of the E–N network (Fig. 1) allows for the calculation of accurate reference areal rainfall against which estimates based on lower density networks may be compared. This network allows the spatial scales to be investigated from 10 × 10 to 100 × 100 km^2. We will first concentrate on the storm rainfall associated to the Mesoscale Convective Complexes (MCCs), as defined by Amani et al. (1996) and Laurent et al. (1997), following Maddox's first definition (1980). Results of a previous work by Lebel and Le Barbé (1997) will be used below to compute climatological standard deviations of estimation errors based on a geostatistical approach. The extension of the study to larger timescales (month, season) will then be explored.

c. A geostatistical framework

The computation of a variance of estimation error requires the inference of a covariance function for the underlying random process. Among the various approaches available to that end, the geostatistical framework is especially convenient because the mean of the process does not need to be estimated. Estimating the mean of the point rainfall process is difficult when working in a limited window. In the case of E–N, for instance, MCCs move eastward at an average speed of 60 km h^{-1} and are thus observed during a few hours only, while their total life duration is more than 10 h and may sometimes reach 48 h or more. Fluctuations of their mean intensity, linked to the diurnal cycle or other factors, may consequently lead to a potentially strong bias in the mean estimation. The reader is referred to Journel and Huijbregts (1978) for a general presentation of geostatistics and to Bacchi and Kottegoda (1995) for a recent synthesis pointing to the interest of using variograms for point and mean areal rainfall estimation purposes. In the geostatistical framework, the variance of estimation error, for a given configuration $\mathcal{C}$ (defined by a network and an estimation area A), is computed as

$$\sigma^2(\mathcal{C}) = -\gamma_{00} - \gamma_{NN} + 2\gamma_{0N}, \tag{4}$$

with

$$\gamma_{00} = \frac{1}{A^2}\int_A\int \gamma(h)\, d^2A,$$

$$\gamma_{NN} = \sum_{i=1}^{N}\sum_{j=1}^{N} \lambda_i\lambda_j\gamma(h_{ij}), \quad \text{and}$$

$$\gamma_{0N} = \sum_{i=1}^{N} \lambda_i \frac{1}{A}\int_A \gamma(h_{ix})\, dA, \tag{5}$$

where h_{ij} is the Euclidean distance between the observation points i and j, h_{ix} is the distance between point i and point x belonging to area A. The variogram of the rainfall field is $\gamma(h)$. The set of weighting coefficients $\{\lambda_i\}$ is the solution of the kriging system.

The variogram may change from one event k to the other if only because the spatial variance of each event is not constant. Thus, $\sigma^2(\mathcal{C})$ is in fact a function of k: $\sigma_k^2(\mathcal{C})$ and the variogram has then to be denoted as γ_k. When many rain fields having approximately similar spatial structures are available, a climatological kriging approach may be considered (Bastin et al. 1984; Lebel et al. 1987). This approach leads to the computation of a scaled variance of estimation error given by

$$\overline{\sigma}^2(\mathcal{C}) = -\overline{\gamma}_{00} - \overline{\gamma}_{NN} + 2\overline{\gamma}_{0N}, \tag{6}$$

where the different terms are the same as in (4); the only difference is that a scaled climatological variogram $\overline{\gamma}(h)$ is now used, which allows the computation of a scaled variance of estimation error, $\overline{\sigma}^2(\mathcal{C})$. For a given event k, $\sigma_k^2(\mathcal{C})$ and $\overline{\sigma}^2(\mathcal{C})$ are related as

$$\sigma_k^2(\mathcal{C}) = s_k^2\overline{\sigma}^2(\mathcal{C}), \tag{7}$$

where s_k^2 is the point variance of the rainfall event k. The climatological standard deviation of estimation error, $\overline{\sigma}^2(\mathcal{C})$ is a measure of the standard estimation error for the configuration $\mathcal{C}$.

The climatological experimental variogram of the Sahelian MCC's event rain fields has been studied by Lebel and Le Barbé (1997), who fitted an exponential model with the following parameters: shape parameter $\beta = 15$ km; nugget $\nu = 15\%$; sill $\alpha = 1$ (since the climatological variogram is the average of scaled realizations, its sill is by definition equal to 1). Of course, the variogram inference involves a sampling error. This error is difficult to assess straightforwardly and we have consequently chosen to account for it in an empirical way—we vary the parameters of the variogram so that some kind of sensitivity analysis may be carried out. Three models will thus be considered: V_1 is a variogram corresponding to fields with the greatest variability ($\beta =$ 10 km; $\nu = 15\%$); V_2 is the variogram proposed by Lebel and Le Barbé (1997); V_3 is a variogram corresponding to smoother fields ($\beta = 15$ km; $\nu = 0\%$). Whereas the areal rainfall estimates are not very sensitive to such fluctuations of the variogram parameters,

the same cannot be said for the estimation variances, as was shown in an example by Lebel and Le Barbé (1997). In such a context where various sources of uncertainties may influence the computation of the standard estimation errors, their validation becomes crucial.

3. Validation of the variance of estimation errors

The aim of the validation is to verify whether the geostatistical approach and the particular model (variogram) used to implement it produce an acceptable assessment of the estimation accuracy for the configuration $\mathcal{C}$. The general idea is as follows. Given a variogram γ_k or $\overline{\gamma}$ and a configuration $\mathcal{C}$, $\sigma_k^2(\mathcal{C})$ or $\overline{\sigma}(\mathcal{C})$ is computed. If $P_k(A)$, the *true rainfall*, were known, then it would be possible to assess how realistic the kriging standard deviations are by computing a set of square deviations between $P_k(A)$ and $\hat{P}_k(A)$ for an array of events ($k = 1, \ldots, K$). But $P_k(A)$ is not known. Authors interested in validation have to rely on very dense rain gauge networks to compute reference areal rain depths supposedly equal to $P_k(A)$. Kriging retains the general idea of validation while avoiding the formal use of $P_k(A)$ in the procedure. This is an important point when only networks of medium density are available.

a. Validation procedure in a geostatistical context

The reference rainfall obtained from the entire network of N^* gauges is noted $P_k^*(A)$, or more simply P_k^*:

$$P_k^* = \sum_{i=1}^{N^*} \lambda_i^* P_{k,i}. \tag{8}$$

It is supposed to be a close representation of $P_k(A)$, but one with sampling errors. Thus, when testing a given configuration $\mathcal{C}$ we have two estimates of $P_k(A)$: P_k^* and $\hat{P}_k(\mathcal{C})$, and we are interested in testing their relative accuracy.

Kriging allows the computation of the theoretical variance of $[P_k^* - \hat{P}_k(\mathcal{C})]$ as

$$\sigma_k^2(\mathcal{C})^* = E\{[P_k^* - \hat{P}_k(\mathcal{C})]^2\} \tag{9}$$

or

$$\sigma_k^2(\mathcal{C})^* = -\sum_{l=1}^{N^*}\sum_{l'=1}^{N^*} \lambda_l^*\lambda_{l'}^*\gamma_k(h_{ll'}) - \sum_{i=1}^{N}\sum_{i'=1}^{N} \lambda_i\lambda_{i'}\gamma_k(h_{ii'}) + 2\sum_{l=1}^{N^*}\sum_{i=1}^{N} \lambda_l^*\lambda_i\gamma_k(h_{li}). \tag{10}$$

In the climatological context defined in (6) and (7), we also have

$$\sigma_k^2(\mathcal{C})^* = s_k^2\overline{\sigma}^2(\mathcal{C})^* \tag{11}$$

with

$$\overline{\sigma}^2(\mathcal{C})^* = -\sum_{l=1}^{N^*}\sum_{l'=1}^{N^*} \lambda_l^*\lambda_{l'}^*\overline{\gamma}(h_{ll'}) - \sum_{i=1}^{N}\sum_{i'=1}^{N} \lambda_i\lambda_{i'}\overline{\gamma}(h_{ii'}) + 2\sum_{l=1}^{N^*}\sum_{i=1}^{N} \lambda_l^*\lambda_i\overline{\gamma}(h_{li}), \tag{12}$$

which is the theoretical climatological reference variance. This reference variance may be directly compared to an accuracy index retrieved from our dataset. This accuracy index is defined as

$$\overline{s}_k^2(\mathcal{C})^* = \left[\frac{P_k^* - \hat{P}_k(\mathcal{C})}{S_k}\right]^2. \tag{13}$$

Indeed, the set of $\{\overline{s}_k^2(\mathcal{C})^*\}$ may be considered as realizations of a random variable $\overline{S}^2(\mathcal{C})^*$, the expectation of which is $\overline{\sigma}^2(\mathcal{C})^*$. Thus, defining

$$\xi^2(\mathcal{C})^* = \frac{1}{K}\sum_{k=1}^{K} \overline{s}_k^2(\mathcal{C})^*, \tag{14}$$

the final validation procedure proposed here compares $\overline{\sigma}^2(\mathcal{C})^*$ and $\xi^2(\mathcal{C})$ for various configurations $\mathcal{C}$, where $\xi^2(\mathcal{C})$ is an experimental variance. The theoretical scaled kriging variance, $\overline{\sigma}^2(\mathcal{C})$, will also be computed.

b. Results

To meet the stationarity condition of kriging, only the group of MCCs accounting for 75% of the annual rainfall in the Sahel according to Laurent et al. (1997) is used. This represents 76 events ($K = 76$) from a total of 133 events recorded during three seasons: 1990, 1991, and 1992. Different configurations are considered. Over the area A_1 (100×100 km^2), four regular networks of decreasing densities correspond to configurations $\mathcal{C}_{11}$, $\ldots$, $\mathcal{C}_{14}$. Over the smaller areas, A_2 (target area of 20×20 km^2) and A_3 (10×10 km^2), only one network of degraded density is built, which corresponds to configurations $\mathcal{C}_{21}$ and $\mathcal{C}_{31}$.

As a starting point the climatological variogram used is model V_2 ($\nu = 15\%$ and $\beta = 15$ km).

1) Area A_1

The four networks are composed of 30, 15, 8, and 4 rain gauges, respectively. In Table 1 are given the values of $\xi(\mathcal{C}_{1j})^*$, $\overline{\sigma}^2(\mathcal{C}_{1j})$, and $\overline{\sigma}^2(\mathcal{C})^*$, ($j = 1, \ldots, 4$). Reference and kriging variances are not so different, but the former are the closest to the experimental variances. Globally, the theoretical variances are in good agreement with the experimental variances.

2) Areas A_2 and A_3

Over these two areas the density of the degraded network (10 gauges over A_2 and 6 gauges over A_3) is half that of the reference network (19 gauges over A_2 and 11 gauges over A_3). In Table 1 note that the kriging

TABLE 1. Experimental variance of estimation error [$\xi(\mathcal{C})^*$] compared to the theoretical reference [$\overline{\sigma}^2(\mathcal{C})^*$] and kriging [$\overline{\sigma}^2(\mathcal{C})$] variances of estimation error defined in (12) and (6), respectively. Values are in percent of the field variance. The climatological variogram used to compute the theoretical variances is an exponential model with nugget = 15% and shape parameter = 10 km.

	Area A_1 (10 000 km^2)				Area A_2 (400 km^2)	Area A_3 (100 km^2)
	$\mathcal{C}_{11}$ 30 gauges	$\mathcal{C}_{12}$ 15 gauges	$\mathcal{C}_{13}$ 8 gauges	$\mathcal{C}_{14}$ 4 gauges	$\mathcal{C}_{21}$ 10 gauges	$\mathcal{C}_{31}$ 6 gauges
Experimental: $\xi^2(\mathcal{C})^*$	13.5	23.8	30.0	40.0	10.5	8.5
Reference: $\overline{\sigma}^2(\mathcal{C})^*$	13.4	19.7	28.5	41.3	12.4	11.6
"True": $\overline{\sigma}^2(\mathcal{C})$	14.5	22.0	30.0	45.0	24.7	27.0

variance is much higher than the reference variance, revealing how misleading a validation procedure would be based on the kriging variance instead of the reference variance. Globally, the reference variances produce the best results. However, the reference variances based on V_2 as compared to the results obtained for A are significantly higher than the experimental variances. Therefore, alternate reference variances are computed using the two other variogram models V_1 and V_3. The variogram corresponding to the smoother spatial structure (exponential with $\nu = 0$ and $\beta = 15$ km) is the one that leads to compute reference variances being the closest to the experimental variances (see Table 2). This illustrates the sensitivity of the theoretical variances of estimation errors to the parameters used for the covariance function, especially over small surfaces (note that in Table 2, the values of the reference variance do not change much for configuration, $\mathcal{C}_1$). Also, the "optimal" variogram is not the same for all the configurations: V_1 gives the best results for configurations $\mathcal{C}_{12}$ and $\mathcal{C}_{13}$, V_2 for $\mathcal{C}_{11}$ and $\mathcal{C}_{14}$, and V_3 for $\mathcal{C}_{21}$ and $\mathcal{C}_{31}$.

At this stage of our study it is possible to formulate a first set of conclusions based on the calibration procedure.

1) For medium-density networks most often available for computing a reference ground truth, there may be a significant difference between the theoretical variance of estimation error computed with respect to the true, but unknown, areal rainfall (here referred to as the kriging variance) and that computed with respect to the available reference rainfall (referred to here as the reference variance). The reference variances must be used for validation purposes (i.e., comparison with experimental variances), while the kriging variances, which are larger than the reference variances, provide (under condition of prior validation) an appropriate measure of the "true" standard estimation error of the areal rainfall for a given measurement configuration.
2) For the scales accessible to the E–N setup (i.e., 100–10 000 km^2), the geostatistical approach produces theoretical variances of estimation errors that are realistic.
3) However, there is a real sensitivity to the parameters of the variogram even when these parameters are varied in the limits allowed by the visual fitting of a model to the experimental variogram. This leads to choosing a "medium" model that will produce the best average validation results over the range of the configuration tested.

TABLE 2. Sensitivity of the reference theoretical variance to changes in the parameters of the climatological variogram. The values in bold are the closest to the experimental variances given in Table 1.

		Area A_1 (10 000 km^2)				Area A_2 (400 km^2)	Area A_3 (100 km^2)
		$\mathcal{C}_{11}$ 30 gauges	$\mathcal{C}_{12}$ 15 gauges	$\mathcal{C}_{13}$ 8 gauges	$\mathcal{C}_{14}$ 4 gauges	$\mathcal{C}_{21}$	$\mathcal{C}_{31}$
V_1	$\nu = 15\%$ $\beta = 10$ km	13.9	**20.8**	**30.2**	43.1	13.4	13.1
V_2	$\nu = 15\%$ $\beta = 15$ km	**13.4**	19.7	28.5	**41.3**	12.4	11.6
V_3	$\nu = 0\%$ $\beta = 15$ km	11.8	17.5	26.2	37.1	**9.6**	**8.3**

Having gained some confidence in the realism of our kriging standard deviations as a measure of the standard estimation errors of the storm areal rainfall in the Sahel, we will now proceed in two directions. First, in section 4, the sensitivity of the standard estimation errors to criteria 1–6 listed at the end of section 2a will be studied. Second, in section 5, we will examine how similar standard errors may be derived for larger timescales such as a month or a season. In order to compare our results to those of other studies a perfectly regular network, shown in Fig. 2, is considered. According to the above conclusions, the variogram used is the exponential model V_2 ($\nu = 15\%$; $\beta = 15$ km), unless explicitly stated otherwise.

4. Relative accuracy of the storm ground truth in the Sahel

a. Fluctuations of the standard estimation error

1) INFLUENCE OF THE AREA OF ESTIMATION AND GAUGE DENSITY

In Fig. 2, the number of gauges is varied for squares of increasing side length (from 10 to 100 km). The networks are composed of 1, 2, 4, 8, and 10 gauges

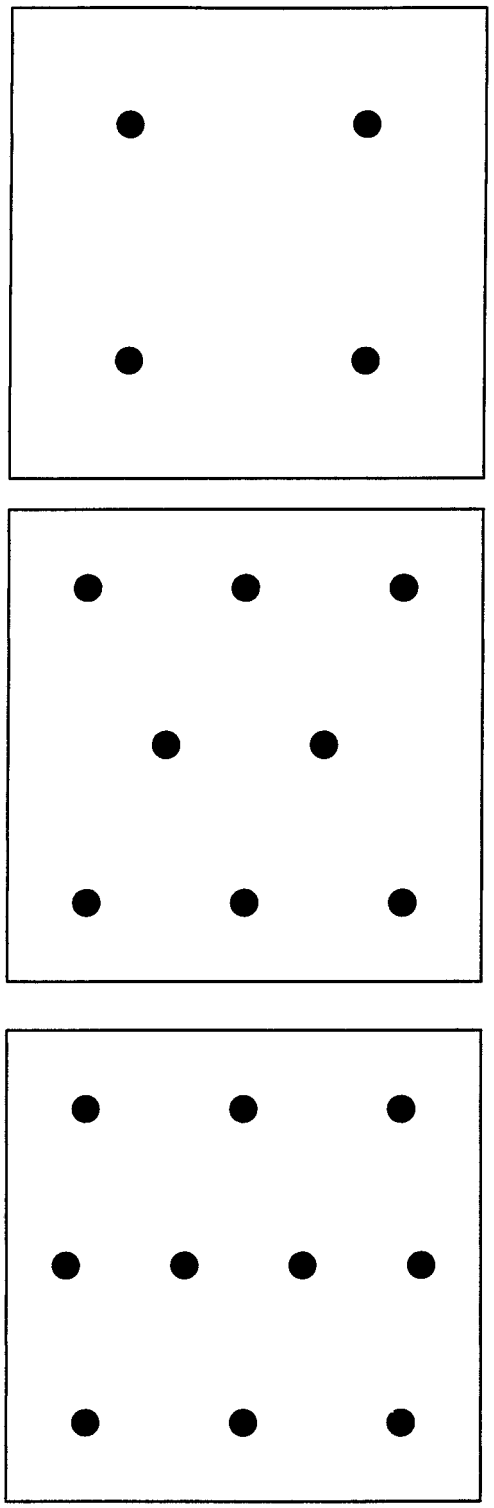

FIG. 2. The theoretical networks used to study the effect of various factors on the standard estimation error of the storm rainfall in the Sahel.

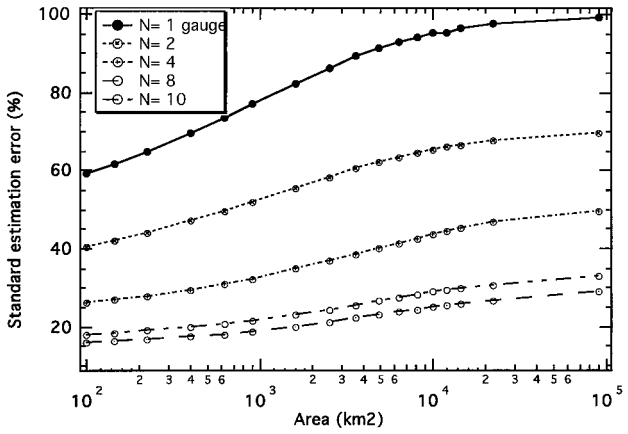

FIG. 3. Variation of the standard estimation error with the estimation area. Five network configurations are tested.

inside a square with side a. The values considered are 10, 20, 30, 40, 50, 60, 80, 90, and 100 km. This gives densities that vary from 10 000 km^2 per gauge to 10 km^2 per gauge. The corresponding climatological kriging standard errors are plotted in Fig. 3.

Figure 4 presents a comparison between E–N standard errors and 1) the standard errors reported in Rodriguez-Iturbe and Meija (1974) for random and stratified rain gauge networks for an exponential covariance function and 2) the standard error as estimated in Zawadzki (1973) in the case of a uniform rain gauge network for an exponantial structure function. The E–N and Zawadzki's results are close to each other, especially for $N = 10$. This was expected since the covariance functions are similar, and Zawadzki (1973) assumed a gauge-to-gauge distance below the decorrelation distance. Ran-

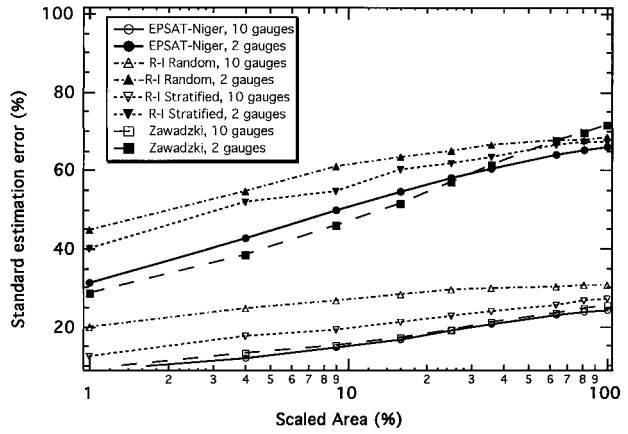

FIG. 4. Comparison of the standard estimation errors of the Sahelian storm rainfall with those computed by Rodriguez-Iturbe and Mejia (1974) and those computed by Zawadzki (1973) for two network configurations. The results obtained by Rodriguez–Iturbe and Mejia (noted R-I) are shown for two different network geometries: random and stratified. The scaled area is the estimation area standardized by the square of the length parameter characterizing the covariance function.

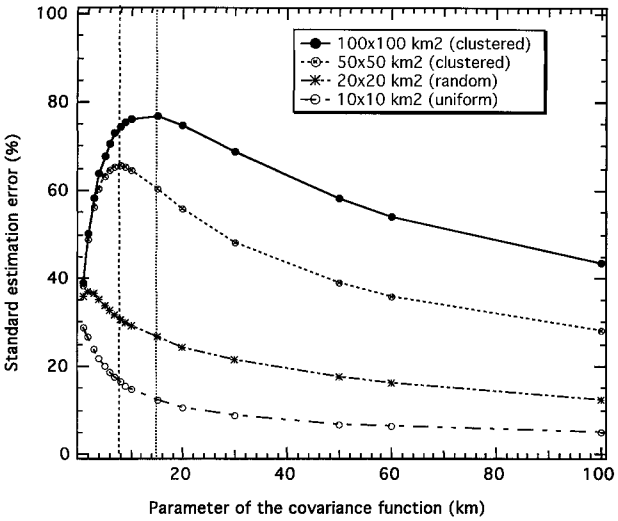

FIG. 5. Effect of the network geometry on the standard estimation error that is tested by using the same target area network while gradually increasing the estimation area. The two vertical lines indicate the position of the maximum of the error function observed for the clustered networks.

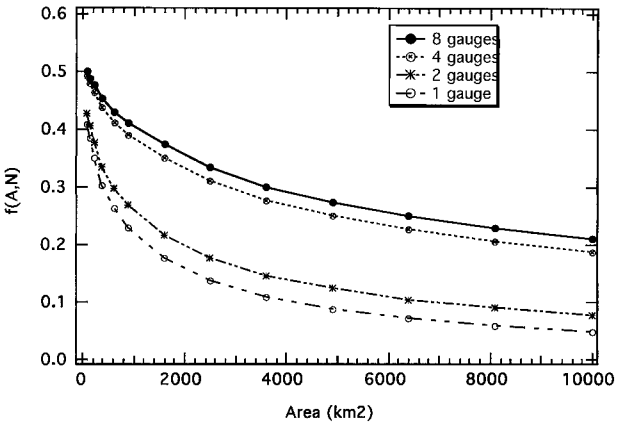

FIG. 6. Experimental values of the function $f(A, N) = 1 - \sqrt{N}\overline{\sigma}(\mathcal{C})$ for four network configurations.

dom networks considered in Rodriguez–Iturbe and Meija (1974) produce errors greater than those corresponding to uniform networks of Zawadzki (1973). The errors associated to stratified networks are intermediate between those of the uniform and of the random configurations.

2) INFLUENCE OF THE NETWORK GEOMETRY

Recently, Morrissey et al. (1995) studied the effect of the network geometry on the standard estimation error. The covariance function selected in their study is exponential. The parameter of the exponential model (the *e*-folding distance) is used as a measure of the spatial structure of the rainfield. It is equivalent to the parameter β of the variogram used here. Morrissey et al. (1995) have shown that, while for random and uniform networks the standard error decreases regularly when the *e*-folding distance is increased, for clustered networks the standard error first increases, then decreases. The maximum is observed for a value of the standardized *e*-folding distance equal to about 0.18 (the *e*-folding distance is standardized by the square root of the averaging area). We have simulated the effect of clustering in the E–N case study by using the dense network of the central target area (Fig. 1). Using only this network for the estimation and gradually increasing the estimation area from the target area to the whole study area is equivalent to progressively transforming a regular network into a clustered network. When the estimation area is limited to the core of the target area (10×10 km^2), the network may be considered as uniform and as random when the estimation area is enlarged to the whole target area (20×20 km^2). Further enlarging the estimation area to 50×50 km^2 and then 100×100 km^2, the network configuration becomes equivalent to that of a clustered network. The results obtained (shown in Fig. 5) are in good agreement with those of Morrissey et al. (1995); the standard error decreases regularly for the estimation areas of 10×10 km^2 and 20×20 km^2. A maximum is observed for $\beta = 8$ km when considering the 50×50 km^2 area (clustered network). The corresponding standardized distance of this maximum is 0.16 (8/50), which is a value close to that of Morrissey et al. (1995). For the 100×100 km^2 area the maximum is observed for $\beta = 15$ km, which corresponds to a standardized distance of 0.15 (15/100).

b. An empirical model for $\overline{\sigma}(\mathcal{C})$

Based on the standard errors calculated from our different hypothetical rain gauge networks, a simple model is presented for the standard estimation error. This model is a function of the two parameters defining the configuration of estimation: the area A and the number of gauges N. Here, $\overline{\sigma}(\mathcal{C})$ can be expressed as

$$\overline{\sigma}(\mathcal{C}) = \frac{1}{\sqrt{N}}[1 - f(A, N)], \qquad (15)$$

where $f(A, N)$ is a decreasing function of A.

The similarity between the curves representing the successive functions $f(A, N)$ when N varies (Fig. 6) suggests plotting $f(A, N)$ as a function of the gauge area A/N (Fig. 7). Over the range of values explored for A ($100 < A < 10\,000$ km^2) and N ($1 < N < 10$ gauges), the following expression,

$$f(A/N) = -0.1683\log(A/N) + 0.717, \qquad (16)$$

can be fitted to the experimental curve with a coefficient of determination of 0.986. Thus, Eq. (15) becomes

$$\overline{\sigma}(\mathcal{C}) = \frac{1}{\sqrt{N}}[0.283 + 0.1683\log(A/N)]. \qquad (17)$$

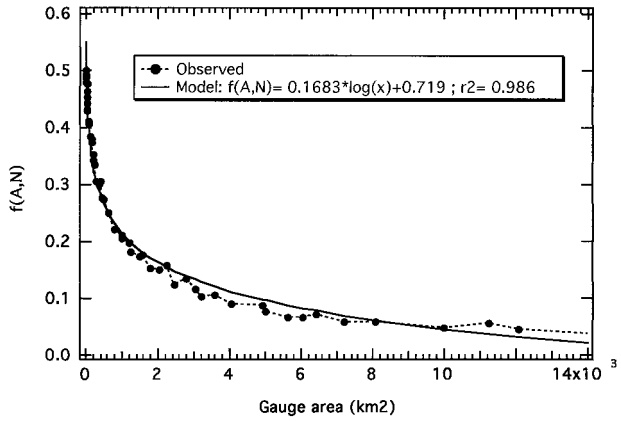

FIG. 7. Values of $f(A, N)$ plotted as a function of the gauge density and fitting a log model.

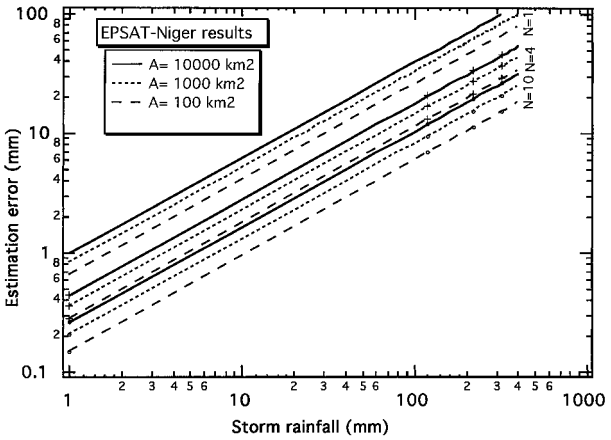

FIG. 8. Absolute estimation error as a function of the storm rainfall.

c. Estimation error as a percentage of the mean

The standard estimation error as given by expression (17) is a convenient criterion for a sensitivity analysis similar to the one carried out above or for a comparison of various estimation configurations, as done in section 3. However, in practice, giving the standard error of mean areal rainfall estimation as a percentage of the mean areal rainfall depth is often more useful. Since the scaling factor used in (7) to define $\overline{\sigma}(C)$ is the standard deviation of the rain field (s_k), the relative estimation error cannot be deduced directly from the standard estimation error. Denoting $e_k(C)$ as the relative estimation error, we have

$$e_k(C) = \frac{s_k \overline{\sigma}(C)}{m_k(A)}, \tag{18}$$

where $m_k(A)$ is the mean storm rain depth for event k over the estimation area A. For the events considered in the validation step of section 3 (MCCs), Lebel and Le Barbé (1997) have shown that a relationship exists between s_k and $m_k(D)$, where $m_k(D)$ is the average raindepth of storm k over the domain of measurement D. This relation is

$$s_k = 1.05 m_k(D)^{0.8}. \tag{19}$$

Note that D is supposed to be larger than A (typically D is in the order of several thousands of square kilometers) so that $m_k(D)$ represents the MCC magnitude at the mesoscale and its estimate is robust. This leads to

$$e_k(C) = 1.05 \frac{\overline{\sigma}(C)}{m_k(A)} m_k(D)^{0.8}. \tag{20}$$

Obviously there is a relation between $m_k(D)$ and $m_k(A)$, but it is partly random and difficult to distinguish. The smaller the value of A as compared to D, the greater the potential difference between $m_k(D)$ and $m_k(A)$. Generally, this additional source of uncertainty in assessing $e_k(C)$ is not taken into account in previous studies. The approximation $m_k(A) = m_k(D)$ (which is true in expectation), gives

$$e_k(C) = 1.05 \overline{\sigma}(C) m_k(D)^{-0.2}, \tag{21}$$

which shows that the relative estimation error is a decreasing function of the storm intensity, as already noted for instance by Huff (1970). Combining expressions (17) and (21) and simplifying $m_k(D)$ into m_k to denote the generic storm magnitude, the error is

$$e_k(C, m_k) = \frac{1.05}{\sqrt{N}} m_k^{-0.2} \left[0.283 + 0.168 \log\left(\frac{A}{N}\right) \right], \tag{22}$$

which provides the relative estimation error as a function of 1) the average raindepth of storm k over the domain of measurement D, 2) the estimation area A, and 3) the number N of gauges over A.

The corresponding numerical values of $e_k(C)$ are given in Fig. 8 for the range of spatial scales investigated here. It is noteworthy that for medium to low density networks such as that considered in this figure, the influence of the number of gauges is stronger than that of the area. For instance, the estimation error is 9.2 mm when estimating an event rainfall of 16 mm (which is the average MCC rainfall in the Sahel) over a 10 000 km^2 with a single rain gauge located at its center. When the area is divided by a factor 10 (10 000 to 1000 km^2), keeping the same number of gauges, the error decreases to 7.6 mm; it decreases to 2.2 mm when the number of gauges is multiplied by a factor of 10 over the same area (10 gauges instead of 1). In both cases, however, the gauge area has been divided by 10 (10 000 to 1000 km^2).

In Fig. 9, the E–N results are compared to those of Huff which, in 1970, gave, for the U.S. Midwest, an error formula similar to ours. After conversion to SI units and taking an average storm duration of 3 h, Huff's formula reads

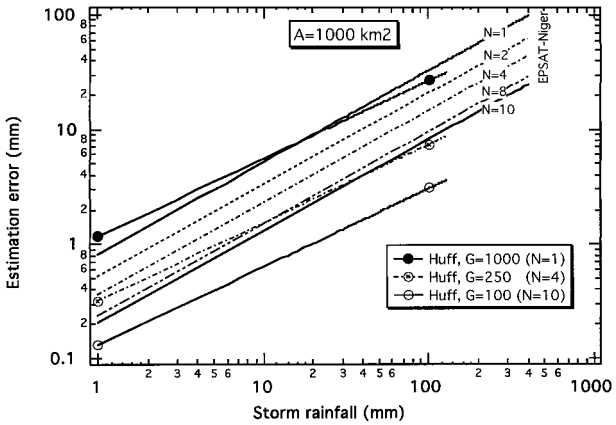

FIG. 9. Comparison of the EPSAT–Niger absolute estimation errors with those reported by Huff (1970) for an estimation area of 1000 km^2.

$$\log[E_k(C, m_k)] = -0.506 + 0.68\log(m_k) + 0.94\log(G) - 0.75\log(A)$$

or

$$\log[e_k(C, m_k)] = -0.506 - 0.32\log(m_k) + 0.94\log(G) - 0.75\log(A), \quad (23)$$

where E denotes an absolute error and e is the relative error as defined in (18).

The values of $e_k(C)$ given by expression (23) have been computed for $A = 1000$ km^2 and $G = \{1000, 250, 100$ km$^2\}$, which is equivalent to $N = \{1, 4, 10\}$. It appears that Huff's results are still more sensitive to the number of gauges than ours. For a similar error of about 7.6 mm when $N = 1$, Huff's error decreases to 0.9 mm when $N = 10$, while the E–N error decreases to 1.9 mm. Another difference between Huff's and E–N's results is that the relative error decreases faster for the Midwest (exponent $= -0.32$) than for the Sahel (exponent $= -0.2$).

5. Estimation errors at larger timescales

a. General expression

We will now focus our attention on larger timescales that are used in satellite validation studies. In such cases, the individual rain depth associated to each event is often not known. The information available would typically be 1) the point cumulative rain depths over the period and 2) the number of storms K that passed over the area (the latter information is retrieved from geostationary satellites).

Supposing the K rainy events to be independent, then the variance for their sum, is

$$\sigma_K^2(C) = \sum_{k=1}^{K} \sigma_k^2(C) = \overline{\sigma}^2(C)\left(\sum_{k=1}^{K} s_k^2\right), \quad (24)$$

where $\sigma_k^2(C)$ $(k = 1, \ldots, K)$ are the variances of estimation for the different events. When $\sigma_k^2(C)$ is standardized by the total rainfall over the K events, $M_K = \sum_{k=1}^{K} m_k$, we get a relative estimation error of M_K, that will be denoted as $E_K(C)$, and which is

$$E_K(C) = \overline{\sigma}^2(C)\frac{\sqrt{\sum_{k=1}^{K} s_k^2}}{\sum_{k=1}^{K} m_k}. \quad (25)$$

Introducing (19) into (24) yields

$$E_K(C) = 1.05\overline{\sigma}(C)\frac{\sqrt{\sum_{k=1}^{K} m_k^{1.6}}}{\sum_{k=1}^{K} m_k}. \quad (26)$$

b. Maximum likelihood approach

Note that $E_K(C)$ is minimum when all the m_k $(k = 1, K)$ are equal to M_K/K. In such a case, denoting M_K/K as m, it becomes

$$E_K(C) = \frac{1.05}{\sqrt{K}}\overline{\sigma}(C)m^{-0.2}, \quad (27)$$

which is similar to expression (21), except for the factor $1/\sqrt{K}$.

This shows that the minimum value of $E_K(C)$ is identical to the relative error for a single event of magnitude m, divided by $K^{1/2}$. In fact, the m_k's are statistically distributed, and a more realistic assessment of $E_K(C)$ will be obtained by considering this distribution. Based on the maximum likelihood principle, the most probable

TABLE 3. Quantiles of the conditional distribution of m_k (expression 37) for a few values of K and corresponding value of CF_K computed with expression (39).

	$k =$										
	1	2	3	4	5	6	7	8	9	10	CF_K
$K = 2$	0.25	0.75									0.749
$K = 3$	0.116	0.315	0.605								0.641
$K = 4$	0.059	0.159	0.291	0.508							0.557
$K = 5$	0.036	0.094	0.167	0.267	0.443						0.501
$K = 10$	0.0079	0.0201	0.0336	0.0488	0.0663	0.0869	0.112	0.145	0.192	0.285	0.362

set of storm rain depths for a given value of K is made of the K quantiles $q(p_k)$ of the distribution when k varies from 1 to K, assuming p_k to be computed as

$$p_k = \frac{k - a}{K + b}(0 \le a \le 1;\ 0 \le b \le 1). \quad (28)$$

Denoting $f(r)$ as the probability density function (PDF) of the event rainfall, the conditional PDF of m_k, (conditional to belonging to a set of K events where their sum is equal to M_K) is given by

$$g(m_k|K, M_K) = 0, \quad \text{for } m_k < 0, \quad \text{or} \quad m_k > M_K,$$

$$g(m_k|K, M_K) = \frac{f(m_k)h(M_K - m_k)}{h(M_K)}, \qquad \text{otherwise}, \quad (29)$$

where h is the PDF of the sum of independent realizations of a random variable with PDF f.

Further assuming that f is exponential (D'Amato and Lebel 1998) with scale parameter s, h is the PDF of the incomplete gamma distribution and it becomes

$$g(m_k|K, M_K) = \frac{\exp(-m_k/s)}{s} \frac{\exp[-(M_K - m_k)/s][(M_K - m_k)/s]^{K-2}}{(n-2)!s} \frac{(n-1)!s}{\exp(-M_K/s)(M_K/s)^{K-1}}, \quad (30)$$

which leads to

$$g(m_k|K, M_K) = (K - 1)\frac{(M_K - m_k)^{K-2}}{(M_K)^{K-1}}. \quad (31)$$

Note that g is independent of the scale parameter of the initial exponential distribution. The cumulative distribution function is then given by

$$G(m_k|K, M_K) = \int_0^{m_k} (K-1)\frac{(M_K - h)^{K-2}}{(M_K)^{K-1}}\, dh \quad \text{and} \quad (32)$$

$$G(m_k|K, M_K) = \frac{(K-1)}{M_K} \int_0^{m_k} \left(1 - \frac{h}{M_K}\right)^{K-2} dh, \quad (33)$$

that is,

$$G(m_k|K, M_K) = 1 - \left(1 - \frac{m_K}{M_K}\right)^{K-1}. \quad (34)$$

The computation of the quantile $m_K(G = p_k)$ is then given by

$$m_k = M_K[1 - (1 - p_k)^{1/(K-1)}]. \quad (35)$$

Introducing (28) into (35), m_k may be written as a function of M_K, the total rainfall over the period considered K, the number of events observed over that period, and the rank k of the observation:

$$m_k = M_K\left\{1 - \left[1 - \frac{(K - k) + a + b}{K + b}\right]^{1/(K-1)}\right\}. \quad (36)$$

Taking $a = 0.3$ and $b = 0.2$ [which is an adaptation of the quantile-unbiased formula proposed by Cunnane (1978)] yields

$$m_k = M_K\left\{1 - \left[1 - \frac{(K - k) + 0.5}{K + 0.2}\right]^{1/(K-1)}\right\}. \quad (37)$$

Thus, varying k from 1 to K in (37), the most probable set of event rain depths $\{m_k\}$ producing a total rainfall M_K is obtained. As an illustration, this set is given in Table 3 for a few values of K. Also given in this table is a correcting factor, CF_K, defined as follows:

$$\mathrm{CF}_K(C) = \frac{E_K(C, M_K)}{e_k(C, M_K/K)}, \quad (38)$$

where $e_k(C, M_K/K)$ is the relative estimation error for an event rainfall of magnitude $m = M_K/K$. The knowledge of the correction factor enables the user to infer the relative estimation error of M_K from that of an event rainfall whose magnitude would be equal to the average m. Combining expressions (21) and (26) [with $m_k(D) = m$ in (21)] it becomes

$$\mathrm{CF}_K = \frac{\sqrt{\sum_{k=1}^{K} m_k^{1.6}}}{M_K^{0.8}K^{0.2}}, \quad (39)$$

showing that CF_K is independent of the network configuration C. Note that if all the m_k's are equal to m, then 39 reduces to

$$\mathrm{CF}_K = \frac{1}{K^{0.5}}. \quad (40)$$

c. Validation

Validation occurs in two steps. First, it is examined whether the combined maximum likelihood and conditional distribution approach allows a realistic assessment of the $\{m_k\}$, $k = 1, K$. To that end, we compare, in Fig. 10:1) the theoretical correction factors, computed with expression (39) for K varying from 1 to 40; 2) the observed correction factors for two years, 1991 and 1992 (in fact, the computation was performed for 1990 as well, producing similar results to those obtained for 1991 and 1992); and 3) the correction factors that would be computed by assuming that all the m_k's are equal to

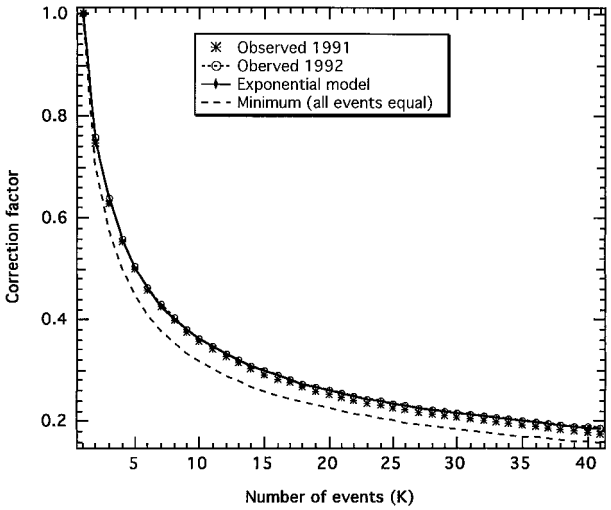

FIG. 10. Comparison of the correction factors computed from expressions (39) (exponential distribution of the storm rain depths) and (40) (all storm rain depths equal to each other) with the experimental values deduced from the EPSAT–Niger observations of 1991 and 1992.

M_K/K, [expression 40]. The correction factors for 1991 and 1992 are averages for moving windows of length K, where K varies from 1 to 41 [i.e., the m_k's observed over a given window K_i introduced in expression (39) to compute $CF_{K_i}^{obs}$]. There is an extremely good agreement between the theoretical curve and the observed curves, while the assumption of all m_k's being equal to M_K/K leads to a significant underestimation of the correction factor, which is an underestimation of the relative estimation error. However, this underestimation is on the order of 10%–15%, which is not so large considering the strong difference in the distribution of the m_k's underlying the two schemes considered here.

The second step of the validation is to compare the theoretical errors to the observed errors in an approach similar to that followed for the validation of the event rainfall errors. For a given value of K, all the K-event rainfall observed in 1990, 1991, and 1992 are calculated, again using a moving window of length K. For four different networks (configurations $\mathcal{C}_{11}$–$\mathcal{C}_{14}$) an observed error (difference between the reference rainfall as defined by expression (8) and the observed rainfall with the configuration under consideration) is then calculated. All the observed errors obtained for a given K are then averaged to provide the average "observed error," $\overline{E_K^{obs}(\mathcal{C})}$ for configuration $\mathcal{C}_{li}$, $i = 1, 4$. These "observed errors" are plotted in Fig. 11 along with their standard deviations and the corresponding modeled errors. The average modeled errors are computed in much the same way as observed errors. For each individual observed error, corresponding to an observed M_K, the theoretical error $E_K(\mathcal{C}, M_K)$ is computed by combining expressions (38) and (39). These theoretical errors are then averaged similarly as done previously for the observed errors, so as to obtain an average "theoretical error," $\overline{E_K^{tho}(\mathcal{C})}$. There is a general trend at overestimating the observed errors with our model (see Fig. 11), which is especially pronounced for the 30-station network, whereas the model performs well for the 15-station network. Performances for the two other networks (four and eight stations, respectively) are intermediate, which means that the network density is apparently not an explanation factor of the performance.

This validation is far from being as reliable as the one carried out at the event scale, given the available samples. However, it shows that for low to medium density networks (those which are of greatest interest to us) our model provides a realistic, even if overestimated, assessment of the relative estimation errors for a K event rainfall.

d. Discussion

We will discuss briefly below the implications of the calculations presented in section 5b and of their validation, presented in section 5c above (numerical examples are given in Table 4). We evaluate typical estimation errors for an average month belonging to the margins of the rainy season (e.g., June, with typically between four and five events per month) and for an average month belonging to the core of the rainy season (e.g., August, with typically a little more than 10 events per month). As a direct consequence of the correction factors shown in Table 3, the relative error will be, on average, divided by a factor of 2 when upscaling from the event to a month of the margins of the rainy season and by a factor of close to 3 when upscaling from the event to a month of the core of the rainy season. Even the simple accumulation of two events significantly reduces the estimation error (the ratio of a two-event error to single-event error is 75%). Networks that are not dense enough at the event scale will rapidly become of an acceptable density when a few events are accumulated. For instance, a network of four gauges uniformly distributed over a 100×100 km^2 area will provide the ground truth with an average uncertainty of less than 15% for the month of June and less than 10% for the month of August, a value that may be deemed acceptable for satellite validation studies. On the other hand, it must be underlined that providing a ground truth with an accuracy better than 10% or even 15% is more challenging when working at the event or 10-day scale since a minimum of 10 gauges is needed over a 100×100 km^2 area. Such a density is easy to reach on *one* $1° \times 1°$ area but, it will take some time, determination, and money before such a network covers the whole Sahel.

6. Conclusions

In a previous paper Lebel and Le Barbé (1997) had shown that, despite the convective nature of the Sahelian rainfall, the structure of the storm rain fields could be

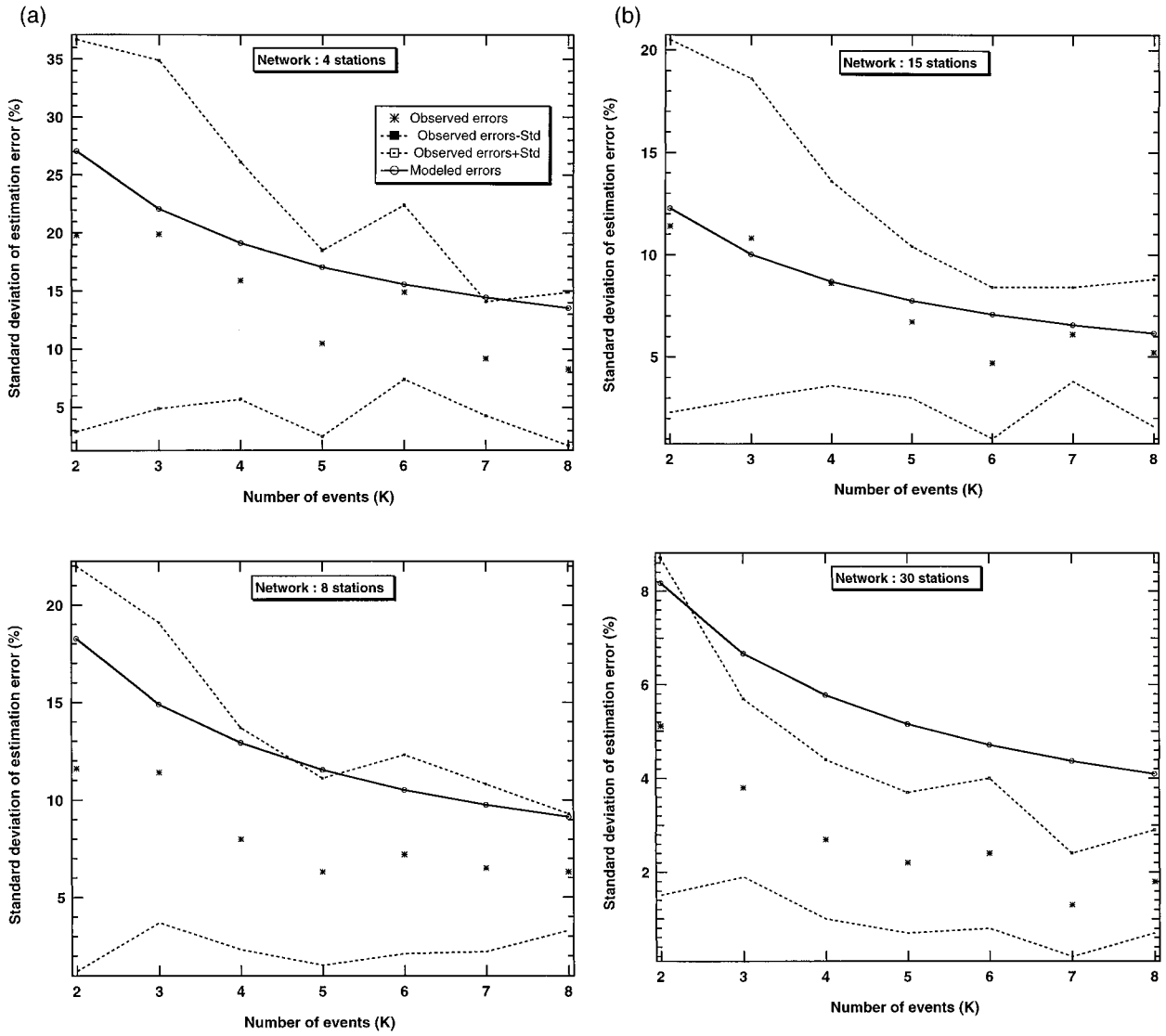

FIG. 11. Relative errors of the areal estimation over a 10 000 km^2 area as a function of the number of independent events for four networks of increasing density. The theoretical values (''modeled errors'') are compared to the observed errors and their standard deviation. The plotted values are averages over the whole range of *K*-event rainfall observed in 1990, 1991, and 1992, where *K* varies from 2 to 8.

represented by a relatively simple exponential model of spatial covariance, at least for scales ranging from a few to a hundred kilometers. The present paper has focused on the validation of the standard estimation errors computed with such a covariance model. Since the reference rain depths used for validation are not the true rain depths but rather estimates, they are tainted with uncertainty and their variance of estimation errors has to be taken into account when computing the theoretical errors that are compared to the experimental errors. When this step is taken, experimental errors compare well with the corresponding errors predicted by the model. This lends some credit to the value of the theoretical kriging variances used to measure the standard estimation errors with respect to the true but unknown storm rain depths. It has to be noted that, over small areas, this latter variance may be as much as twice the variance computed with respect to the reference rain depths.

Using an empirical relationship between the mean and the variance of the storm rain fields, standard estimation errors have been converted into relative errors. A sensitivity analysis to various parameters (network geometry, network density, size of the estimation areas) has confirmed and upgraded the results obtained for other regions of the world, either from models or experimental studies. Over an area of 1000 km^2, the relative error decreases from 45% to 11% for a storm rainfall of 20 mm, and from 37% to 9% for a storm rainfall of 50 mm, when increasing the number of gauges from 1 to

TABLE 4. Absolute (mm) and relative (%) estimation errors for three regular networks covering a 100 × 100 km² area and three values of K. The number of observed events, $K = 5$ and $K = 10$, represent the approximate average number of events in Jun and Aug, respectively. For $K > 1$, two estimates of the error are given: one from expression (39) and the other from expression (40).

ML approach	Event (16 mm)	Average Jun (80 mm) 5 events; $CF_5 = 0.5$		Average Aug (160 mm) 10 events; $CF_{10} = 0.36$	
1 gauge	9.2 mm 58%	23 mm	29%	34 mm	21%
All events equal		20 mm	25%	29 mm	18%
4 gauges	4.1 mm 26%	10.3 mm	13%	15 mm	9.3%
All events equal		9.3 mm	11.5%	13 mm	8.2%
10 gauges	2.2 mm 14%	5.5 mm	6.9%	8 mm	4.9%
All events equal		5.0 mm	6.3%	7.1 mm	4.0%

10, provided the network geometry is uniform. The Sahelian values obtained for a single-gauge network are very similar to those computed by Huff (1970) in Illinois; they are significantly larger for denser networks. Also, the relative error decreases more slowly with the increase of the storm rainfall in the Sahel than in the midwestern portion of the United States.

An extension of the computation of relative estimation errors has been proposed for larger time steps, that is, when several storm rain depths are accumulated. Assuming an exponential distribution of the storm rain depth for the Sahelian MCCs and after computation of the conditional PDF of the K-event rainfall, a theoretical expression has been derived that allows the retrieval of the K-event rainfall estimation error from that of the corresponding event rainfall of same average magnitude. The errors provided by this expression compare relatively well to the observed errors, except for our denser validation network (30 stations over a 10 000 km² area), which indicates that, when increasing progressively the density, good reference estimates are obtained faster in reality than expected by the geostatistical model.

Some basic lessons may be retrieved from this study regarding the estimation of the ground truth for the validation of satellite estimates or GCM outputs in the Sahel. At the storm scale and for any estimation area between 100 and 10 000 km², 10 gauges uniformly spaced over the estimation area are a minimum to obtain reference rain depths with an average error on the order of less than 10% for a 100 km² area and of less than 15% for a 10 000 km² area. Relative errors are decreased by about 70% to 80% when shifting from the event scale to the 10-day scale.

At the monthly scale, it appears that the average error associated to estimations computed with the denser parts of the operational networks (which have a density of about 2000 km² per gauge in the southern part of Niger for instance) is around 10% (9% in August for a 2000 km² per gauge network and 13% in June) for an estimation area of 10 000 km². Nevertheless, with such a density, this error may be as high as 15% for below average monthly rainfall.

To sum up, if estimation units of 1° × 1° (or 12 000 km²) are targeted, a density of approximately 1000 to 1200 km² per gauge is a minimum to obtain reliable estimates of the event or 10-day areal rainfall under average conditions of rain. At the monthly scale, a density of 2000 to 2500 km² per gauge is both a minimum and reasonable target to obtain reliable estimates of the areal rain depths all over the Sahel. Such densities could be reached at no great expense and will ensure a valuable complement to the costly satellites that are targeted for improving the rainfall monitoring over the Tropics.

On the other hand, for hydrological or agronomical studies interested in smaller areas (typically 100 to 1000 km²), far denser networks are required, involving specific means that operational networks will be unable to provide before long.

Since the areas considered here are 1° × 1° and below, a comparison with results obtained in previous studies for other regions of the world is difficult. As a matter of fact, studies motivated by satellite validation of global climatology projects most often concentrate on larger spatial scales such as 2.5° × 2.5° or 5° × 5°. An attempt at comparing our results to those presented in Graves et al. (1993) shows that for an identical gauge area of 10 000 km² the monthly rainfall estimation error over a 5° × 5° box was estimated at 10.5%, 12.5%, and 20% for Pre-STORM (Oklahoma), GATE (tropical Atlantic), and Texas, respectively. As may be seen in our Table 4, for the same gauge area, the error for the Sahel is in the order of 21%–29%, depending on the monthly rainfall, but this figure applies to a 1° × 1° box. Further work is thus needed to extend the results presented here to larger spatial scales.

REFERENCES

Amani, A., T. Lebel, J. Rousselle, and J. D. Taupin, 1996: Typology of rainfall fields to improve rainfall estimation in the Sahel by the area threshold method. *Water Resour. Res.,* **32,** 2473–2487.

Bacchi, B., and N. T. Kottegoda, 1995: Identification and calibration of spatial correlation patterns of rainfall. *J. Hydrol.,* **165,** 311–348.

Bastin, G., B. Lorent, C. Duqué, and M. Gervers, 1984: Optimal estimation of the average areal rainfall and optimal selection of rain gauge locations. *Water Resour. Res.,* **20,** 463–470.

Bell, T., A. Abdullah, R. L. Martin, and G. R. North, 1990: Sampling errors for satellite-derived tropical rainfall: Monte Carlo study using a space–time stochastic model. *J. Geophys. Res.,* **95,** 2195–2206.

Cunnane, C., 1978: Unbiased plotting positions—A review. *J. Hydrol.,* **37,** 205–222.

D'Amato, N., and T. Lebel, 1998: On the characteristics of the rainfall events in the Sahel with a view to the analysis of climatic variability. *Int. J. Climatol.*, **18,** 955–974.

Desbois, M., 1994: TROPIQUES, a small satellite for the study of the variability of water and energy cycles in the intertropical band. Preprints, *European Symp. on Satellite Remote Sensing,* Rome, Italy, SPIE, 14–17.

Flitcroft, I. D, J. R. Milford, and G. Dugdale, 1989: Relating point to area average rainfall in semiarid West Africa and the implications for rainfall estimations derived from satellite data. *J. Appl. Meteor.*, **28,** 252–266.

Graves, C. E., J. B. Valdes, S. S. P. Shen, and G. R. North, 1993: Evaluation of sampling errors of precipitation from spaceborne and ground sensors. *J. Appl. Meteor.,* **32,** 374–385.

Huff, F. A., 1970: Sampling errors in measurement of mean precipitation. *J. Appl. Meteor.,* **9,** 35–44.

Journel, A. G., and C. I. Huijbregts, 1978: *Mining Geostatiscs.* Academic Press, 597 pp.

Laurent, H., T. Lebel, and J. Polcher, 1997: Rainfall variability in Soudano–Sahelian Africa studied from rain gauges, satellite and GCM. *Proc. 13th Conf. on Hydrology of the 77th AMS Annual Meeting,* Long Beach, CA, Amer. Meteor. Soc., 17–20.

Lebel, T., and L. Le Barbé, 1997: Rainfall monitoring during HAPEX-Sahel: 2. Point and areal estimation at the event and seasonal scales. *J. Hydrol.*, **188–189,** 97–122.

——, G. Bastin, C. Obled, and J. D. Creutin, 1987: On the accuracy of areal rainfall estimation: A case study. *Water Resour. Res.*, **23,** 2123–2134.

——, J. D. Taupin, and M. Gréard, 1995: Rainfall monitoring: The EPSAT-Niger set-up and its use for Hapex-Sahel. *Hydrologie et Météorologie de Méso-Echelle dans HAPEX-Sahel: Dispositif de Mesures au Sol et Premiers Résultats,* T. Lebel, Ed., ORSTOM, 31–68.

Le Roux, X., J. Polcher, G. Dedieu, J.-C. Menaut, and B. Monteny, 1994: Radiation exchanges above West African moist savannas: Seasonal patterns and comparison with a GCM simulation. *J. Geophys. Res.*, **99,** 25 857–25 868.

Li, Q., R. L. Bras, and D. Veneziano, 1996: Analysis of Darwin rainfall data: Implications on sampling strategy. *J. Appl. Meteor.*, **35,** 372–385.

Maddox, R. A., 1980: Mesoscale convective complexes. *Bull. Amer. Meteor. Soc.*, **61,** 1374–1387.

Morrissey, M. L, J. A. Maliekal, J. S. Greene, and J. Wang, 1995: The uncertainty of simple spatial averages using rain gauge networks. *Water Resour. Res.*, **31,** 2011–2017.

North, G. R, and S. Nakamato, 1989: Formalism for comparing rain estimation designs. *J. Atmos. Oceanic Technol.*, **6,** 985–992.

Peters-Lidard, C. D, and E. F. Wood, 1994: Estimating storm areal average rainfall intensity in field experiments. *Water Resour. Res.,* **30,** 2119–2131.

Rodriguez-Iturbe, I., and J. M. Mejia, 1974: The design of rainfall networks in time and space. *Water Resour. Res.,* **10,** 713–728.

Seed, A., and G. L. Austin, 1990: Variability of summer Florida rainfall and its significance for the estimation of rainfall by gages, radar and satellites. *J. Geophys. Res.*, **95** (D3), 2207–2215.

Silverman, B. A, and L. K. Rogers, 1981: On the sampling variance of raingage networks. *J. Appl. Meteor.,* **20,** 1468–1478.

Simpson, J., R. F. Adler, and G. R. North, 1988: A proposed Tropical Measuring Mission (TRMM) satellite. *Bull. Amer. Meteor. Soc.*, **69,** 278–295.

Valdes, J. B., E. Ha, C. Yoo, and G. R. North, 1994: Stochastic characterisation of space–time precipitation: Implications for remote sensing. *Adv. Water Resour.,* **17,** 47–59.

Woodley, W. L., A. R. Olsen, A. Herndon, and V. Wiggert, 1975: Comparison of gauge and radar methods of convective rain measurement. *J. Appl. Meteor.,* **14,** 909–928.

Zawadzki, I., 1973: Errors and fluctuations of rain gauge estimates of areal rainfall. *J. Hydrol.,* **18,** 243–255.